Monte Carlo study of carrier-light coupling in terahertz quantum cascade lasers

Christian Jirauschek[1, a)]

Emmy Noether Research Group "Modeling of Quantum Cascade Devices", Institute for Nanoelectronics, Technische Universität München, D-80333 Munich, Germany

We present a method for self-consistently including the optical cavity field into Monte Carlo-based carrier transport simulations. This approach allows for an analysis of the actual lasing operation in quantum cascade lasers, considering effects such as gain saturation and longitudinal mode competition. Simulation results for a terahertz quantum cascade laser are found to be consistent with experiment.

PACS numbers: 42.55.Px, 73.63.Hs, 78.70.Gq

The development of innovative types of quantum cascade lasers (QCLs) and subsequent design optimization has gone hand in hand with detailed modelling, involving more and more sophisticated simulation tools.[1–10] Especially in the terahertz regime, there is still plenty of room for improvement of the structures, for example in terms of output power, efficiency and temperature performance.[11] In this context, detailed carrier transport simulations have proven very useful, accounting for inter- and intrasubband processes alike and yielding not only level occupations, but also kinetic carrier distributions within each of the levels. Well-established approaches include the semiclassical ensemble Monte Carlo (EMC) method,[1–7] and quantum transport simulations based on the density matrix[8] or non-equilibrium Green's functions formalism.[9,10] Notably, these simulations have up to now almost exclusively focused on the carrier transport, completely neglecting the optical cavity field. An exception is a Monte-Carlo-based study of the coupled cavity dynamics and electron transport, however only considering carrier interaction with photons and phonons.[12] Carrier transport simulations allow for an analysis of the unsaturated optical gain, indicating if the investigated QCL structure will lase at all under the assumed conditions. However, no statements about the actual lasing operation, including the emitted optical power, the electric current and the carrier distributions, can be made. Evidently, an inclusion of the lasing action in the simulation would be desirable for many practical reasons, above all the device optimization with respect to the output power and wall-plug efficiency. Furthermore, such an analysis could provide insight into the carrier dynamics on a microscopic level, yielding an improved understanding of the light-matter interaction in such devices. In the following, we introduce an approach which allows for a straightforward implementation of the laser field into EMC simulations, without a significant increase of the numerical load. The presented scheme considers the coupled cavity field and carrier transport dynamics in a completely self-consistent manner, accounting for effects such as gain saturation and longitudinal mode competition. We present simulation results for a terahertz QCL, which are found to be consistent with experimental data.

Induced optical transitions between an initial and a final level, in the following denoted by i and j, are commonly described in terms of a spectral power gain coefficient $g_{ij}(\omega)$ and the population change associated with the induced emission and absorption events,[13]

$$g_{ij}(\omega) = \frac{\omega_{ij}}{|\omega_{ij}|}\frac{\pi\omega Z_0}{V n_0 \hbar}|d_{ij}|^2 (p_i - p_j)\mathcal{L}_{ij}(\omega), \quad (1a)$$

$$\partial_t p_i|_{\mathrm{ind}} = I\frac{\pi Z_0}{n_0 \hbar^2}|d_{ij}|^2 (p_i - p_j)\mathcal{L}_{ij}(\omega). \quad (1b)$$

Here, $g_{ij}(\omega) > 0$ corresponds to gain, and $g_{ij}(\omega) < 0$ indicates loss. The constants Z_0 and $\hbar$ denote the impedance of free space and reduced Planck constant, respectively. V and n_0 are the volume and refractive index of the gain medium. The line shape as a function of the angular optical frequency ω is given by

$$\mathcal{L}_{ij}(\omega) = \frac{1}{\pi}\frac{\gamma_{ij}}{\gamma_{ij}^2 + (\omega - |\omega_{ij}|)^2}, \quad (2)$$

where γ_{ij} and $\omega_{ij} = (E_i - E_j)/\hbar$ denote the optical linewidth and resonance frequency of the transition. $E_{i,j}$ and $p_{i,j}$ are the level eigenenergies and occupations, and d_{ij} is the corresponding transition matrix element. Furthermore, I denotes the optical intensity.

In a semiclassical EMC simulation, the carrier transport is modeled by a stochastic evaluation of the inter- and intrasubband scattering events for a large ensemble of discrete particles. Each carrier is at a given time described by its quantum state $|i_n, \mathbf{k}_n\rangle$ (which then has an occupation $p = 1$), where i_n denotes the subband and $\mathbf{k}_n$ is the in-plane wave vector of the nth carrier, with $n = 1, \dots, N$. In such simulations, the physical quantities are typically computed from the corresponding ensemble averages. The total gain is obtained from Eq. (1a) by summing over all carriers n and all available final states $|j, \mathbf{k}_n\rangle$ with conserved in-plane wave vector $\mathbf{k}_n$,

$$g(\omega) = \frac{\pi Z_0 \omega}{V n_0 \hbar}\sum_{n,j}\frac{\omega_{i_n j}}{|\omega_{i_n j}|}|d_{i_n j}|^2 \mathcal{L}_{i_n j}(\omega). \quad (3)$$

a)Electronic mail: jirauschek@tum.de;
http://www.nano.ei.tum.de/noether

For periodic structures like QCLs, it is appropriate to evaluate transitions from states within a single central period to the available final states (also including those in adjacent periods). The simulated volume is then given by $V = L_\mathrm{p}N/n_\mathrm{s}$, where L_p and n_s are the period length and the sheet doping density per period.

In EMC simulations, all scattering processes are evaluated based on quantum mechanically calculated Boltzmann-like scattering rates. The contribution from optically induced transitions can be computed from Eq. (1b). To account for effects such as mode competition and multimode lasing, we have to sum over all relevant longitudinal modes, characterized by their frequencies ω_m and intensities I_m. For a carrier sitting in state $|i, \mathbf{k}\rangle$, the transition rate to a state $|j, \mathbf{k}\rangle$ with occupation probability $f_{j\mathbf{k}}$ thus becomes

$$r_{i \rightarrow j} = \frac{\pi Z_0}{n_0 \hbar^2} |d_{ij}|^2 (1 - f_{j\mathbf{k}}) \sum_m I_m \mathcal{L}_{ij}(\omega_m). \quad (4)$$

In principle, in EMC simulations the photon dynamics can be evaluated in analogy to the carrier transport, by stochastic sampling of the discrete photon population in each relevant mode.[12] However, the statistical fluctuations associated with the rare photon emission events make it difficult to obtain sufficient accuracy.[12] Such problems are here avoided by using classical intensities I_m rather than discrete photon populations. The intensity evolution over a time interval δ can be described by

$$I_m(t + \delta) = I_m(t) \exp\left([\Gamma(\omega_m) g(\omega_m) - a(\omega_m)] c\delta/n_0\right), \quad (5)$$

where $c\delta/n_0$ is the propagation distance of the light in the gain medium during that time. In Eq. (5), δ has to be chosen short enough that $g(\omega_m)$ can be considered constant. Γ denotes the confinement factor, c is the vacuum speed of light, and $a = a_\mathrm{m} + a_\mathrm{w}$ is an effective loss coefficient containing both the mirror and waveguide loss.[14] The description of outcoupling losses by a distributed coefficient a_m is very common,[14] and works especially well for moderate output coupling at the facets. Interference effects between adjacent modes and counterpropagating waves are not considered in our approach. Such effects can become relevant for the multimode dynamics and coherent instabilities in modelocked lasers.[15]

Our self-consistent 3D EMC simulation includes all the essential scattering mechanisms, also accounting for Pauli's exclusion principle.[7] Carrier-carrier interactions are implemented based on the Born approximation, taking into account screening in the full random phase approximation.[4] Also considered is scattering with impurities as well as acoustic and longitudinal-optical phonons, including nonequilibrium phonon effects. Interface roughness is implemented assuming typical values of 0.12 nm for the mean height and 10 nm for the correlation length.[7] We simulate four periods of the structure, using periodic boundary conditions for the first and last period.[2] The optical cavity dynamics is considered by including the photon-induced scattering contribution,
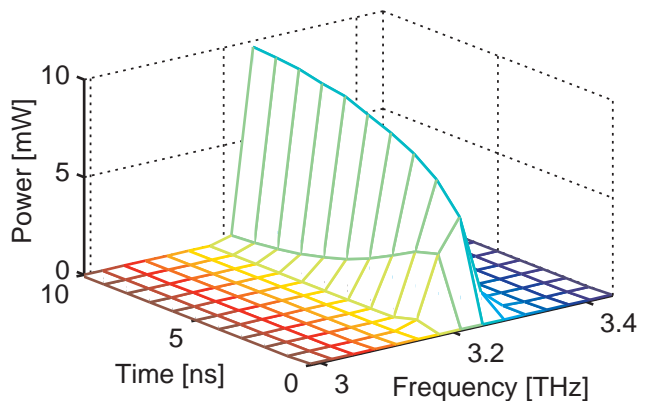

FIG. 1. (Color online) Temporal evolution of the outcoupled power P_m^out at different longitudinal mode frequencies f_m.
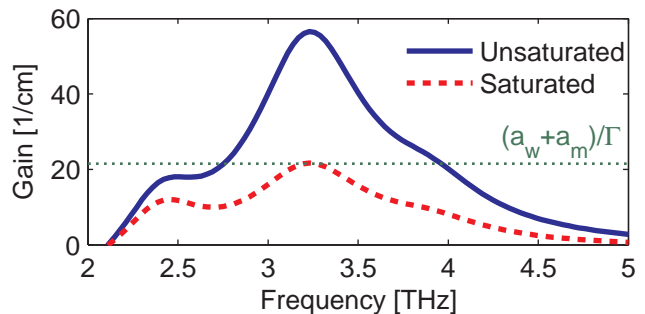

FIG. 2. (Color online) Unsaturated and saturated power material gain coefficient vs frequency. For comparison, the cavity loss is also indicated.

Eq. (4), in the carrier transport simulation and updating $g(\omega_m)$ and I_m for each considered mode after sufficiently short time intervals δ, using Eqs. (3) and (5). The homogeneous linewidth in Eq. (2) is self-consistently calculated based on lifetime broadening.[7] Stimulated emission and absorption do not affect the optical coherence; the corresponding scattering events are thus ignored in the linewidth calculation. Inhomogeneous gain broadening arises if transitions at different frequencies contribute to the gain spectrum, which can result in multimode operation. The subband energies and wave functions are obtained by solving the Schrödinger–Poisson (SP) equation.[16] The EMC and SP simulations are then performed iteratively until convergence is reached.

To validate our simulation approach, we compare the results to experimental data for a 3.0 THz resonant phonon depopulation design, consisting of 178 periods.[14] For this structure, comprehensive temperature resolved experimental data are available, along with detailed specifications of the device, including the optical cavity. The cavity length and gain medium cross section are $L = 1.22$ mm and $A = 178 \times 0.0539\,\mu\mathrm{m} \times 23\,\mu\mathrm{m}$, respectively, and the facet reflectivity is $R = 0.85$; furthermore, $n_0 = 3.8$, $a_\mathrm{w} = 18.7\,\mathrm{cm}^{-1}$, $a_\mathrm{m} = 1.3\,\mathrm{cm}^{-1}$, and $\Gamma = 0.93$.[14] First, the structure is investigated for a lat-
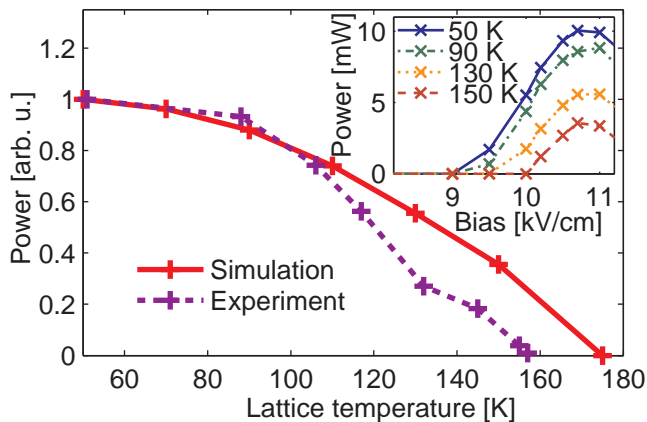
FIG. 3. (Color online) Simulated and measured maximum outcoupled optical power vs temperature. The inset shows the simulated optical power vs the applied bias for different lattice temperatures T_L.

tice temperature of $T_L = 50\,\mathrm{K}$ at a bias of $10.7\,\mathrm{kV/cm}$, where our simulation yields the maximum output power. We consider modes between 2.5 THz and 3.5 THz, with a frequency spacing of $df = c/(2Ln_0) = 0.0324\,\mathrm{THz}$. They are seeded with a small initial intensity ($I_m\,(t=0) = 313\,\mathrm{W/cm^2}$). For moderate outcoupling, the single facet power of a mode at frequency $f_m = \omega_m/(2\pi)$ is obtained as $P_m^{\mathrm{out}} = \frac{1}{2}I_m A\,(1-R)/\Gamma$, where the factor $\frac{1}{2}$ arises because I_m encompasses both the forward and backward propagating wave in the cavity. In Fig. 1, the temporal evolution of P_m^{out} is shown for 15 of the modes, centered around the gain maximum. After a time of $10\,\mathrm{ns}$, the lasing operation has nearly reached steady state, yielding a stationary output power of $10.0\,\mathrm{mW}$ which is basically accumulated in a single mode. This is in agreement with the experimentally observed predominant single-mode behavior of this structure.[14] The corresponding experimental value, measured at a heat sink temperature $T_s = 11\,\mathrm{K}$[17] and uncorrected for the collection efficiency of the Winston cone used in the measurement setup, is $2.6\,\mathrm{mW}$.[14] With an estimated collection efficiency of around 30%,[18] this value corresponds to the simulation result. The unsaturated (solid line) and saturated (dashed line) spectral gain profiles are shown in Fig. 2, and the cavity loss is also indicated for comparison (dotted line). As expected for stationary lasing, the peak saturated gain is clamped at the cavity loss.

Multimode simulations, as presented in Fig. 1, are computationally quite tedious, since long simulation times are required to reach steady state. Thus, in the following, we a priori assume single-mode operation as experimentally observed,[14] considering in our simulation only the mode with the maximum gain. In Fig. 3, the maximum outcoupled optical power (normalized to its value at 50 K) is shown as a function of the lattice temperature T_L, comparing simulation results (solid line) to experimental temperature resolved measurements (dashed line).[14,17] The overall agreement is

good, with a slight deviation between the simulated and measured maximum operating temperatures (175 K vs 158 K), which we mainly attribute to uncertainties in the exact value of a_w.[14] The experimental structure lases best at around $13\,\mathrm{V}$ for all temperatures.[14] Also the simulation yields a temperature insensitive optimum bias which is located at around $10.7\,\mathrm{kV/cm}$ (see the inset of Fig. 3), corresponding to a voltage drop of $10.3\,\mathrm{V}$ across the active region of the investigated structure. This difference between the theoretical and experimental value can largely be explained by additional parasitic voltage drops in the experimental structure, especially in the contacts.[6] We have also successfully tested our approach for various other designs, such as a 4.4 THz high power QCL.[19]

In conclusion, a method is presented to straightforwardly include the optical cavity field into self-consistent EMC carrier transport simulations, allowing for the analysis of the actual lasing operation in QCLs. Effects like gain saturation, gain clamping and mode competition are naturally accounted for. Comparisons to experimental data confirm the validity of our approach.

[1] R. Köhler, R. C. Iotti, A. Tredicucci, and F. Rossi, Appl. Phys. Lett. **79**, 3920 (2001).
[2] R. C. Iotti and F. Rossi, Appl. Phys. Lett. **78**, 2902 (2001).
[3] H. Callebaut, S. Kumar, B. S. Williams, Q. Hu, and J. L. Reno, Appl. Phys. Lett. **84**, 645 (2004).
[4] O. Bonno, J.-L. Thobel, and F. Dessenne, J. Appl. Phys. **97**, 043702 (2005).
[5] X. Gao, D. Botez, and I. Knezevic, J. Appl. Phys. **101**, 063101 (2007).
[6] C. Jirauschek, G. Scarpa, P. Lugli, M. S. Vitiello, and G. Scamarcio, J. Appl. Phys. **101**, 086109 (2007).
[7] C. Jirauschek and P. Lugli, J. Appl. Phys. **105**, 123102 (2009).
[8] R. C. Iotti and F. Rossi, Phys. Rev. Lett. **87**, 146603 (2001).
[9] R. Nelander, A. Wacker, M. F. Pereira, D. G. Revin, M. R. Soulby, L. R. Wilson, J. W. Cockburn, A. B. Krysa, J. S. Roberts, and R. J. Airey, J. Appl. Phys. **102**, 113104 (2007).
[10] T. Kubis, C. Yeh, P. Vogl, A. Benz, G. Fasching, and C. Deutsch, Phys. Rev. B **79**, 195323 (2009).
[11] B. S. Williams, Nat. Photonics **1**, 517 (2007).
[12] R. C. Iotti and F. Rossi, Rep. Prog. Phys. **68**, 2533 (2005).
[13] R. W. Boyd, *Nonlinear Optics* (Academic, New York, 2003).
[14] B. S. Williams, S. Kumar, Q. Hu, and J. L. Reno, Opt. Express **13**, 3331 (2005).
[15] C. Y. Wang, L. Diehl, A. Gordon, C. Jirauschek, F. X. Kärtner, A. Belyanin, D. Bour, S. Corzine, G. Höfler, M. Troccoli, J. Faist, and F. Capasso, Phys. Rev. A **75**, 031802 (2007).
[16] C. Jirauschek, IEEE J. Quantum Electron. **45**, 1059 (2009).
[17] Here we assume $T_L = T_s + 40\,\mathrm{K}$, as experimentally determined for $T_L = 158\,\mathrm{K}$.[14] $T_L - T_s$ mainly depends on the dissipated electric power, which has been found to be relatively constant over the relevant temperature range for operation at optimum bias.[14]
[18] A. Tredicucci, R. Köhler, L. Mahler, H. E. Beere, E. H. Linfield, and D. A. Ritchie, Semicond. Sci. Technol. **20**, 222 (2005).
[19] B. S. Williams, S. Kumar, Q. Hu, and J. L. Reno, Electron. Lett. **42**, 89 (2006).